An efficient maximum power point tracking architecture for weakly coupled piezoelectric harvesters based on the source I-V curve

Nicolas Decroix, Pierre Gasnier, Adrien Badel

An Efficient Maximum Power Point Tracking Architecture for Weakly Coupled Piezoelectric Harvesters based on the source I-V curve

Nicolas Decroix
Univ. Grenoble Alpes, CEA, LETI,
MINATEC, F-38000 Grenoble, France
Univ. Savoie Mont Blanc, SYMME,
F-74000 Annecy, France
nicolas.decroix@cea.fr

Pierre Gasnier
Univ. Grenoble Alpes, CEA, LETI,
MINATEC, F-38000 Grenoble, France
pierre.gasnier@cea.fr

Adrien Badel
Univ. Savoie Mont Blanc, SYMME,
F-74000 Annecy, France
adrien.badel@univ-smb.fr

***Abstract*— This paper describes a novel Maximum Power Point Tracking (MPPT) architecture for weakly coupled piezoelectric harvesters. It is based on a new algorithm, called the I-V curve algorithm for Current-Voltage curve. It enables a fast calculation of the optimal electrical loads for different extraction techniques like Standard Energy Harvesting (SEH) and parallel/series Synchronized Switch on Inductor (p/sSSHI) without requiring any open circuit measurement on the piezoelectric harvester. This architecture has been validated thanks to Simulink simulations. Optimal loads are obtained after 1.5 mechanical period and the obtained electrical power is always greater than 90% of the optimal power.**

I. INTRODUCTION

Vibration energy harvesting is a promising candidate for powering wireless sensor nodes for IoT. However, the power output of these harvesters heavily depends on the input mechanical conditions (vibrations amplitude and frequency) as well as the unavoidable harvester's variations due to its aging or environment variation (temperature variation mainly). To convert vibration into electricity, piezoelectric-based harvesters are very attractive for their high power density at small scale [1] and their high output voltages as compared with electromagnetic converters. Piezoelectric energy harvesters (PEH) are classically qualified as weakly or strongly electromechanically coupled. This paper focuses on the weakly coupled ones. Working with weakly coupled harvesters can be a first step to test algorithms without the effect of the mechanical part.

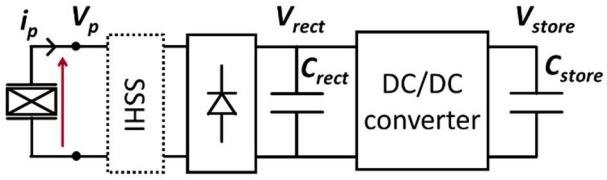

Figure 1 : Typical architecture for piezoelectric energy harvesting with the SEH, pSSHI or sSSHI extraction technique

A commonly used architecture for PEH is the Standard Energy Harvesting technique (SEH). This architecture is composed of a rectifier and a smoothing capacitor C_{rect} (Fig. 1). It can be upgraded with an inversion stage for the so-called Synchronized Switch Harvesting on inductor (SSHI). It is called parallel (pSSHI) or series (sSSHI) depending on the position of the inductance in the circuit. It has been demonstrated in many works that nonlinear techniques like SSHI harvest more energy than SEH, even for self-supplied circuits [2,3]. These techniques are very efficient provided that the voltage V_{rect} or the input resistance of the DC/DC converter is regulated to an optimal value. Power management circuits with dedicated electronic architectures and algorithms should then be developed for constantly tracking the maximum power point (MPPT). These intelligent circuits are indeed mandatory for most harvesting extraction strategies. [4].

There are different categories of MPPT algorithms that can work for different harvesting techniques. For weakly coupled harvesters, perturb and observe (P&O) [5,6] and fractional open circuit voltage (FOCV) [7,8] algorithms are mainly used thanks to their simplicity and ease of implementation. P&O algorithms constantly adapt the control setting of the implemented technique according to an increase or decrease of the harvested power. In [5], a P&O algorithm is implemented with a buck-boost converter based on output power measurements (on V_{store} in Fig. 1) over a few mechanical cycles. In [6], the only setting of the system is the ratio of the capacitor divider of the voltage measurement, which changes the voltage current ratio managed by the MPPT algorithm. P&O algorithms are often slow to reach the maximum power because they incrementally change their control and have to wait for the settlement of the measured quantity. For their part, FOCV algorithms are based on a periodic measurement of the piezoelectric voltage in open circuit condition [7]. For very weakly coupled harvesters, the maximum power is reached when the output DC voltage V_{rect} is equal to half the open circuit voltage. Nevertheless, FOCV algorithms require the piezoelectric harvester to be in open circuit for a minimum of half a mechanical period which does not allow to transfer power during that time. Moreover, algorithms trying to regulate an optimal voltage (on V_{rect}) are not efficient as this voltage value is no longer the optimal one if the input vibration amplitude changes.

To overcome this drawback, a few works propose to estimate the optimal resistive load and performs the regulation of that load with a DC/DC converter in discontinuous-conduction mode. In [9], Xia et al. calculates the optimal input load of a DC/DC converter. There algorithm is launched periodically and finds the optimal load thanks to the voltage information given when regulating two different loads. The second regulated load is non-optimal and is applied only for the measurement process. The speed of the algorithm is hence not optimal as a non-optimal load is applied and the system might not harvest the optimal power during that time. In [6] the P&O algorithm regulates a load so the system is amplitude vibration independent as well.

In this paper, we propose a new architecture and algorithm called the I-V curve algorithm that seeks and sets the optimal

load of a weakly coupled piezoelectric harvester in a fast and efficient way. It enables to extract the maximum power even if the amplitude vibration varies. This algorithm is also independent of the harvesting techniques used in this paper SEH, pSSHI and sSSHI. Being able to change between harvesting techniques can help improving the efficiency of the energy conversion of a DC/DC converter, and thus optimizing the whole harvesting chain. In this work, we focus on frequency and amplitude varying accelerations.

Section II. describes the piezoelectric model, the architecture linked to the MPPT algorithm and its concept. Section III. presents temporal simulations of the proposed architecture based on commercially available off-the-shelf (COTS) components.

II. OPTIMAL LOAD MEASUREMENT CONCEPT

A. Model and schematic

When the electromechanical coupling is low, the electrical side of the piezoelectric harvester has no impact on its mechanical part, the PEH can then be modeled with an ideal sinusoidal current source of amplitude I_0 and frequency f_{mec} in parallel with a capacitor C_p as it can be seen on Fig. 2.

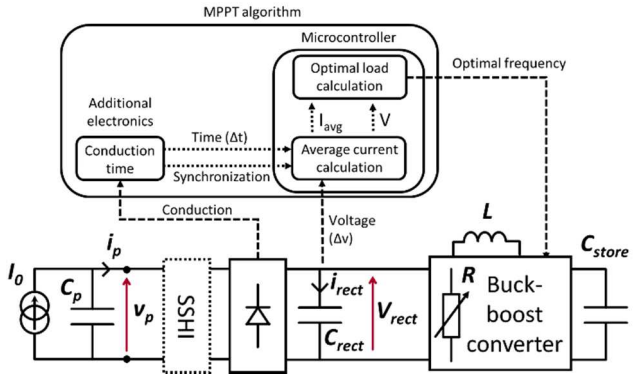

Figure 2 : Architecture of the proposed I-V curve algorithm and its associated circuit

The work presented in this paper is based on simulations only (LTSpice and Matlab/Simulink/Simscape electrical). Fig. 2 shows some of the hardware used in the simulation. A negative voltage converter (NVC) [3] is used as a rectifier. The DC/DC converter used is a buck-boost converter in discontinuous-conduction mode (DCM) to perform the resistive impedance matching. The buck-boost technology is used thanks to the independence of its input voltage V_{rect} with the input resistance R when used in DCM. Indeed, the relation between its input resistance and the control of the associated switch is given by Eq. (1).

$$R = 2L/f_{sw}t_1^2 \quad (1)$$

L is the inductance of the buck-boost, f_{sw} is the control frequency of the switch and t_1 is the on time of the switch. The dotted SSHI box represents a possible SSHI-like inversion switch, including its inductance.

B. Theory

Our optimal load measurement method is based on four voltage measurements across the smoothing capacitor C_{rect}. The average current flowing through C_{rect} ($I_{avg} = C_{rect}\frac{\Delta V_{rect}}{\Delta t}$) and the voltage V_{rect} are determined for half a mechanical period with two voltage measurements. The same two measurements are performed a second time at another operating point (for another mechanical half period). This way, we can plot two points A and B on the average current versus voltage graph (Fig. 2). The characteristic of the source seen before C_{rect} (PEH and rectifier) being linear, point A and B allow to find the current I-V curve of the harvester associated with the current extraction method. The points crossing the x-axis and the y-axis, rectified voltage and average current respectively, are the open circuit voltage V_{OC} and short circuit average current I_{SC} of the source seen before capacitor C_{rect}. The current optimal load is then calculated by dividing the open circuit voltage V_{OC} and the short circuit average current I_{SC} measured for the current harvesting technique, as given in Eq. (2).

$$R_{opt_{technique}} = V_{OC_{technique}}/I_{SC_{technique}} \quad (2)$$

This method works for the three following techniques : SEH, pSSHI and sSSHI. The three source characteristics can be seen on Fig. 3. The load obtained with this method is more accurate if point A and B are far from each other but by doing this, these two points can get far from the optimal voltage (i.e. half the open circuit voltage $V_{OC}/2$). An optimum has to be found between the accuracy of the load measurement and the relative distance to the optimal voltage.

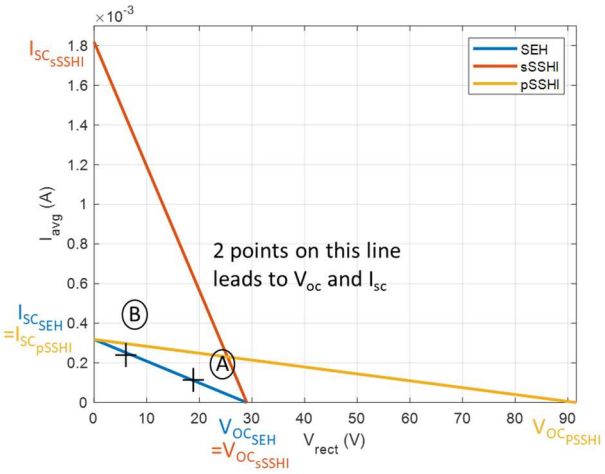

Figure 3 : Theoretical current voltage characteristic of PEH seen by C_{rect} (I_0 = 500µA for SEH and pSSHI; I_0=300µA for sSSHI, f_{mec} = 30Hz)

Contrary to [11], which uses the I-V graph to evaluate the open circuit voltage to set the optimal $V_{OC}/2$ voltage on V_{rect}, our method proposes a simple, fast and efficient way to evaluate the current optimal load thanks to the open circuit voltage V_{OC} and the average short circuit.

C. Proposed implementation

Our method operates in two successive phases (phase A and B corresponding to points A and B in Fig. 3. Each phase uses two voltage measurements : V_{A1} and V_{A3} or V_{B5} and V_{B7} for phase A and B respectivelly, as shown in Fig 4. An example in the case of a SEH technique can be seen on Fig. 4. It also shows the timing of the 4 voltage measurements and the activation of the DC-DC leading to the voltage drop ΔV_{DC-DC} between phase A and B. From 0s to 0.4s, a non-optimal load is regulated by the DC-DC from the beginning of the simulation. At point 1, the NVC is conducting until point 2 which means current is flowing to the capacitor C_{rect} during this period. At point 3, the DC-DC converter is used to reduce

the voltage (ΔV_{DC-DC}) so the points A and B on the current-voltage graph are not too close. Voltage measurements V_{A1} and V_{A3} (ΔV_{rect}) are taken at point 1 and 3 as the calculated average current is valid only for half a mechanical period. The time difference Δt is also measured between point 1 and 3 thanks to a conduction angle measurement (see next section) The voltage difference between point 3 and 4 (ΔV_{DC-DC}) is an adjustable parameter and has been set to 4V in the simulation shown in Fig. 4. The same process is operated between point 5 and point 7 (V_{A5} and V_{A7}).

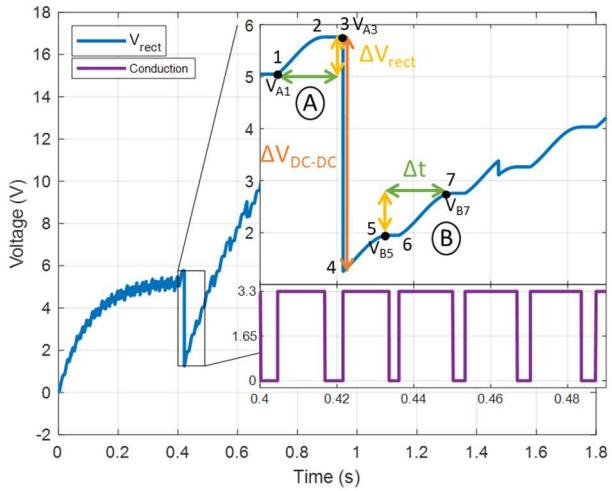

Figure 4 : Simulink simulation of the proposed "I-V curve method" applied in the case of a SEH technique (I_0 = 500µA, f_{mec} = 30Hz, C_p = 90 nF, C_{rect}= 6 µF)

One should notice that the choice of the capacitor C_{rect}, its tolerance, the amplitude I_0 and the voltage jump ΔV_{DC-DC} will have an impact on the accuracy of the measurement. Indeed, for a fixed amplitude I_0 and frequency f_{mec}, a small capacitor value will allow a fast rise of V_{rect} which increases the voltage difference before and after the conduction (between V_{A1} and V_{A2} for example). For a practical and low power analog to digital conversion (e.g 12 bit ADC resolution), a high difference between V_{A1} and V_{A3} allows to precisely measure the resulting ΔV_{rect} and in fine obtain a precise average current evaluation.

A large voltage drop ΔV_{DC-DC} allows a reasonable spacing between points A and B (Fig. 3), which can compensate for the possible inaccuracy of the average current evaluation. Moreover, the resolution of the ADC will also have an impact on the estimated load as the resolution is finite. A possible way of overcoming the inaccuracy of the average current measurement would be to measure the current on several mechanical periods but we will not address it in this paper.

III. Simulations

The proposed algorithm and architecture has been simulated temporally in order to verify its functionality in operation. The voltage and conduction time measurements functions implemented on these simulations are depicted in Fig. 5 and detailed in the following sections.

A. Voltage measurements

For those simulations, a 12 bit analog to digital converter has been chosen to perform the voltage measurements. This type of ADC is currently used in practical low power applications such in as microcontroller based architecture [8]. Moreover, an 11-bit effective resolution ADC has been chosen to take the possible noise into account. A voltage divider ratio of 1/50 is used to measure V_{rect}, leading to a maximum measurable voltage of 61.2V (the internal voltage reference microcontroller's ADC is 1.224V in our case).

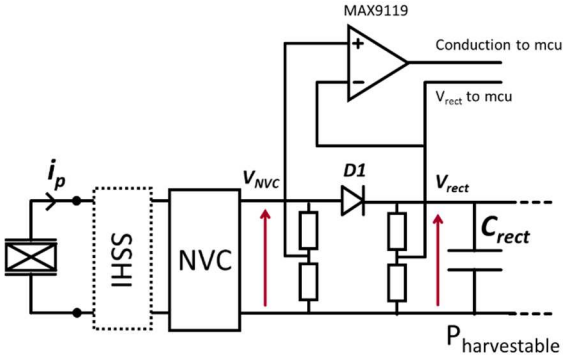

Figure 5 : Hardware associated with the proposed "I-V curve method"

B. Conduction time

The conduction time is performed by comparing the voltage difference between the two ports of the diode connected between capacitor C_{rect} and the output of the NVC, in a similar way as [12]. We use here a very low-power comparator MAX9119. With COTs component, this diode is often mandatory with an NVC in order to block reverse current. The conduction signal goes high when the rectifier conducts ($V_{NVC} > V_{rect}$) and it goes low when the rectifier stops conducting ($V_{NVC} < V_{rect}$). Fig. 6 shows the simulation (LTSpice) of the conduction time measurement with the MAX9119 comparator and its surrounding components.

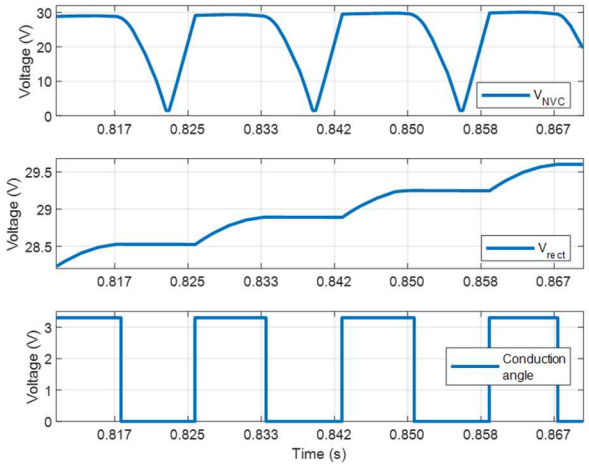

Figure 6 : Waveforms of conduction time measurement (LTSpice Simulation)

The use of this type of comparator for very low power, autonomous and cold-start compliant power management circuits has been demonstrated in many previous works [2].

C. Temporal simulation

In this section, a more complete temporal simulation of the proposed system is performed by varying three types of parameter successively: three amplitude variations (from I_0 =500µA to 700µA and 300µA), one mechanical frequency variation (f_{mec} = 30Hz to 60Hz) and a change of extraction technique during the simulation (from SEH to sSSHI) as it can be seen on Fig. 7 d). The MPPT algorithm is launched five times, at t=1s, 3s, 5s, 7s and 9s (x-axis ticks of the plots)

meaning that the two measurement phases (2x2 voltage measurements) are performed, followed by an update of the optimal load. Fig. 7 shows the voltages, loads and powers versus time. The blue curves corresponds to the theoretical optimal values and the black curves are the effective values reached by our system. Fig. 7 c) is the harvestable electrical power, i.e. the electrical power harvested in C_{rect}. It means that an additional conversion efficiency of the DC-DC must therefore be taken into account.

One can note that at the simulation startup, the effective input load of the DC-DC converter has been intentionally set to a non-optimal value with respect to the input parameters. Nevertheless, the optimal load is obtained a few mechanical cycles after the MPPT algorithm is launched. This simulation shows that, every time the algorithm is launched, a load close to the optimal one is found and the power obtained is greater than 90% of the maximum harvestable electrical power. We clearly see the interest of evaluating the optimal load instead of an optimal voltage since the obtained load only depends on the mechanical frequency or the extraction technique and does not depend on the vibration amplitude.

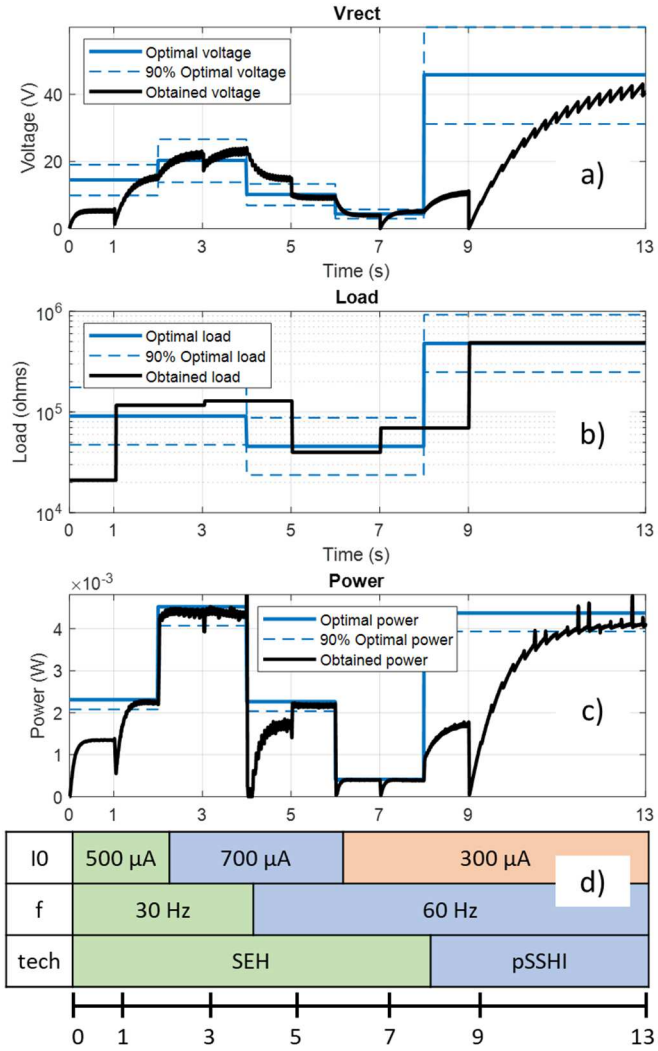

Figure 7 : Simulink Simulation showing the temporal evolution of waveforms of the proposed algorithm (C_p = 90 nF, C_{rect}= 6 µF)

IV. Conclusion

This work shows a new MPPT algorithm that helps tracking the maximum power point of weakly coupled PEH. This method is rather simple and relies on four voltage measurements on a smoothing capacitor. This method permits fast MPPT tracking (1.5 mechanical period) compared to P&O algorithm. Energy is still harvested while the tracking is performed. Obtaining an optimal load is also preferable to an optimal voltage so that the regulation of the MPP is vibration amplitude independent. Hence, this algorithm performance is a tradeoff between P&O and FOCV algorithms. Moreover, this algorithm works seamlessly for different harvesting techniques like SEH or pSSHI.

Perspectives of this algorithm are first its implementation on a real hardware as all the work in this paper is based on simulations. The compatibility with the mechanical model of a PEH will also need to be addressed as mechanical transients are not taken into account in this paper. Methods that enhance the accuracy of the average current calculation should also be addressed in the future.

References

[1] Roundy SJ. Energy scavenging for wireless sensor nodes with a focus on vibration to electricity conversion PhD Thesis Berkeley Berkeley, CA: University of California; 2003.

[2] S. Boisseau, P. Gasnier, M. Gallardo, and G. Despesse, "Self-starting power management circuits for piezoelectric and electret-based electrostatic mechanical energy harvesters," *Journal of Physics*, p. 6, 2013.

[3] A. O. Badr, E. Lou, Y. Y. Tsui, and W. A. Moussa, "A High Efficiency AC/DC NVC-PSSHI Electrical Interface for Vibration-Based Energy Harvesters," *IEEE Transactions on Circuits and Systems I: Regular Papers*, vol. 67, no. 1, pp. 346–355, Jan. 2020.

[4] A. Brenes, A. Morel, J. Juillard, E. Lefeuvre, and A. Badel, "Maximum power point of piezoelectric energy harvesters: a review of optimality condition for electrical tuning," Smart Mater. Struct., vol. 29, no. 3, p. 033001, Mar. 2020.

[5] S. Li, A. Roy, and B. H. Calhoun, "A Piezoelectric Energy-Harvesting System with Parallel-SSHI Rectifier and Integrated MPPT Achieving 417% Energy-Extraction Improvement and 97% Tracking Efficiency," in 2019 Symposium on VLSI Circuits, Jun. 2019, pp. C324–C325.

[6] J. Sankman and D. Ma, "A 12-µW to 1.1-mW AIM Piezoelectric Energy Harvester for Time-Varying Vibrations With 450-nA \bm Q," IEEE Transactions on Power Electronics, vol. 30, no. 2, pp. 632–643, Feb. 2015.

[7] M. Shim, J. Kim, J. Jeong, S. Park, and C. Kim, "Self-Powered 30 µW to 10 mW Piezoelectric Energy Harvesting System With 9.09 ms/V Maximum Power Point Tracking Time," IEEE Journal of Solid-State Circuits, vol. 50, no. 10, pp. 2367–2379, Oct. 2015.

[8] N. Kawai, Y. Kushino, and H. Koizumi, "MPPT controled piezoelectric energy harvesting circuit using synchronized switch harvesting on inductor," in *IECON 2015 - 41st Annual Conference of the IEEE Industrial Electronics Society*, Nov. 2015, pp. 001121–001126.

[9] H. Xia, R. Chen, L. Ren, and Q. Zhou, "Direct calculation of source impedance to adaptive maximum power point tracking for broadband vibration energy harvesting," Journal of Intelligent Material Systems and Structures, vol. 28, no. 9, pp. 1105–1114, May 2017.

[10] Y. Hu, I. Chen, and T. Tsai, "A piezoelectric vibration energy harvesting system with improved power extraction capability," in 2016 IEEE Asian Solid-State Circuits Conference (A-SSCC), Nov. 2016, pp. 305–308.

[11] J. Leicht and Y. Manoli, "A 2.6 µW – 1.2 mW Autonomous Electromagnetic Vibration Energy Harvester Interface IC with Conduction-Angle-Controlled MPPT and up to 95% Efficiency," *IEEE Journal of Solid-State Circuits*, vol. 52, no. 9, pp. 2448–2462, Sep. 2017.